NUMERICAL SIMULATION OF TWO-DIMENSIONAL HEAT CONVECTION-DIFFUSION WITH ELLIPSOID GEOMETRIES

Contents

Abstract. Ever wonder what's the how to keep your warm bath at the right temperature while helping the environment? This paper introduces and analyzes two-dimensional heat convection-diffusion through the Navier-Stokes formulation of fluid-flow and the classical heat equation. Our mission is to determine the optimal amount of water necessary to maintain the perfect bathtub temperature. BLAH BLAH BLAH

1. Introduction

The basis of this paper is to develop a model that permits a person to maintain their preferred temperature of the bathtub water while minimizing water consumption.

2. Model overview

Throughout this work we will denote the spatial region under scrutiny by $\Omega \subseteq \mathbb{R}^2$, and we write $\partial\Omega$ to indicate the boundary of the region. The function $T : \Omega \times \mathbb{R}_{\geq 0} \to \mathbb{R}$ will denote the temperature $T = T(x, y, t)$, and the functions $v_x : \Omega \times \mathbb{R}_{\geq 0} \to \mathbb{R}$ and $v_y : \Omega \times \mathbb{R}_{\geq 0} \to \mathbb{R}$ will denote $v_x = v_x(x, y, t)$ the horizontal and $v_y = v_y(x, y, t)$ the vertical components of the velocity of the fluid flow.

2.1. Two-dimensional Navier-Stokes formulation.

The Navier-Stokes equations for an incompressible fluid are given by

$$\nabla \cdot v = 0 \tag{1}$$

$$\frac{\partial v}{\partial t} + (v \cdot \nabla)v = -\frac{1}{\rho}\nabla p + \alpha \nabla^2 v \tag{2}$$

where $v = (v_x, v_y)$ is the fluid velocity, ρ denotes mass density of the fluid, and p denotes pressure. Incompressibility is incorporated through Equation (), since nonzero divergence implies the presence of either sources or sinks of fluid. Now because v is two-dimensional,

Date: February 1, 2016.

Equation () actually implies a pair of partial differential equations for both the x and y components. The pressure p is determined through the Poisson equation

$$\nabla^2 p = b, \tag{3}$$

where b is taken as a constant term for the purposes of this study. Many wonderful resources exist online for understanding the formulation of these equations, specifically Barba's work [5], but we do not include a derivation of these relations here.

2.2. **Heat convection-diffusion equation.** The heat convection-diffusion equation found in the literature [3],

$$\frac{\partial T}{\partial t} - \alpha \nabla^2 T + v \cdot \nabla T = 0, \tag{4}$$

is a combination of parabolic and hyperbolic partial differential equations relating the temporal change in temperature with its spatial diffusion and the flow of heat packets elsewhere in the fluid. Here, ∇ is the gradient operator $\left(\frac{\partial}{\partial x}, \frac{\partial}{\partial y}\right)$, ∇^2 denotes the Laplacian $\frac{\partial^2}{\partial x^2} + \frac{\partial^2}{\partial y^2}$, $v = (v_x, v_y)$ denotes the fluid velocity vector, and α is a diffusivity constant.

The ubiquity of parabolic PDEs in modeling scientific phenomenon is well known, since it captures the essence of diffusive processes. Elliptic PDEs often arise out of physical environments with a present potential field (e.g. gravitational or electrostatic), or in the cases of incompressible fluid flow [3, 1]. We use the latter for motivating this model, as bathtub water exhibits the standard characteristics of incompressible fluid.

2.3. **Numerical methods.** We proceed by providing a brief overview of the numerical methods used in this study. To approximate the solution to a PDE, we discretize the region Ω under consideration into a coordinate mesh. For convention, we write $T^n_{i,j}$ to denote the temperature at the (i, j) mesh coordinate at the time interval $t = n$.

Modifying the notation employed by Ames [1], we establish the following nomenclature for the numerical operations in the model (the use of T is without loss of generality and can be substituted for v and p as well):

$$\begin{aligned}
\overrightarrow{\Delta}_i T^n_{i,j} &= T^n_{i+1,j} - T^n_{i,j} && \text{Forward differencing} \\
\overleftarrow{\Delta}_i T^n_{i,j} &= T^n_{i,j} - T^n_{i-1,j} && \text{Backward differencing} \\
\overleftrightarrow{\Delta}_i T^n_{i,j} &= T^n_{i+1/2,j} - T^n_{i-1/2,j} && \text{Central differencing}
\end{aligned}$$

The estimation of partial derivatives using the above techniques result in different rates of convergence as the numerical increment decreases. In particular, we have

$$\frac{\partial T^n_{i,j}}{\partial x} = \frac{\overrightarrow{\Delta}_j T^n_{i,j}}{\Delta x} + O(\Delta x), \tag{5}$$

(while we use differentiation along the horizontal axis, the convergence is without loss of generality of axis), and we similarly have

$$\frac{\partial T^n_{i,j}}{\partial x} = \frac{\overleftarrow{\Delta}_j T^n_{i,j}}{\Delta x} + O(\Delta x), \tag{6}$$

while for central differencing, we have

$$\frac{\partial T^n_{i,j}}{\partial x} = \frac{\overleftrightarrow{\Delta}_j T^n_{i,j}}{\Delta x} + O((\Delta x)^2). \tag{7}$$

Indeed, as $\Delta x \to 0$ we see that central differencing has a quadratic rate of convergence, while forward and backward differencing are linear. For this advantage we employ central differencing in computing spatial derivatives. However, as the time evolution is simulated on the fly, we cannot have access to $T_{i,j}^{n+1}$ when computing $T_{i,j}^{n}$. We consequently use backward differencing to estimate the time derivative.

The approximated Navier-Stokes equations now read

$$\frac{\overleftrightarrow{\Delta}_j (v_x)_{i,j}^n}{\Delta x} + \frac{\overleftrightarrow{\Delta}_i (v_y)_{i,j}^n}{\Delta y} = 0 \tag{8}$$

(9)

$$\frac{\overleftarrow{\Delta}_n v_{i,j}^n}{\Delta t} + (v_x)_{i,j}^n \frac{\overleftrightarrow{\Delta}_j (v_x)_{i,j}^n}{\Delta x} + (v_y)_{i,j}^n \frac{\overleftrightarrow{\Delta}_i (v_y)_{i,j}^n}{\Delta y} = -\frac{1}{\rho}\left(\frac{\overleftrightarrow{\Delta}_j p_{i,j}^n}{\Delta x} + \frac{\overleftrightarrow{\Delta}_i p_{i,j}^n}{\Delta y}\right) + \alpha\left(\frac{\overleftrightarrow{\Delta}_j{}^2 (v_x)_{i,j}^n}{(\Delta x)^2} + \frac{\overleftrightarrow{\Delta}_i{}^2 (v_y)_{i,j}^n}{(\Delta y)^2}\right).$$

The Poisson equation is

$$\frac{\overleftrightarrow{\Delta}_j{}^2 p_{i,j}^n}{(\Delta x)^2} + \frac{\overleftrightarrow{\Delta}_i{}^2 p_{i,j}^n}{(\Delta y)^2} = b. \tag{10}$$

Finally, heat convection-diffusion is given by

$$\frac{\overleftarrow{\Delta}_n T_{i,j}^n}{\Delta t} - \alpha\frac{\overleftrightarrow{\Delta}_j{}^2 T_{i,j}^n}{(\Delta x)^2} + \frac{\overleftrightarrow{\Delta}_i{}^2 T_{i,j}^n}{(\Delta y)^2} + (v_x)_{i,j}^n \frac{\overleftrightarrow{\Delta}_j T_{i,j}^n}{\Delta x} + (v_y)_{i,j}^n \frac{\overleftrightarrow{\Delta}_i T_{i,j}^n}{\Delta y} = 0 \tag{11}$$

The algorithmic approach we take is as follows. Using the numerical formulas given above, isolate the time derivative and set its value to the other side of the equation. In the case of temperature, for example, we then update its value with

$$T_{i,j}^{n+1} \leftarrow T_{i,j}^n + \Delta t \cdot \frac{\partial T_{i,j}^n}{\partial t}. \tag{12}$$

This pattern is used throughout the computer implementation of these models. The remaining question is the stability of these results. In fact, as we shall discuss in Section 4, these equations can be highly unstable, especially with a naive assignment of parameter values.

2.4. **Bathtub optimization problem.** The goal of this study is to identify a process through which the avid bather may seek to achieve uniform water temperature, ideally wasting as little water as possible. Using the aforementioned numerical models to simulate bathtub dynamics, we propose an optimization problem by which to approach this goal. Let t_{total} indicate the period in which the faucet is turned on, let T_{f} denote the temperature of the water in the faucet, and let $V(t)$ denote the total volume of water that has left the faucet. We assume that $\frac{dV}{dt} = c$, i.e., the strength of the faucet is fixed at a chosen c throughout the duration of the bath. Now, consider the surface integral

$$f_{\text{cont}}(t) = \int_\Omega |T(x, y, t) - T_{\text{f}}| \; d\omega. \tag{13}$$

We propose the minimization problem

$$\arg\min_c \int_0^{t_{\text{total}}} V(t)\, dt \quad \text{such that} \quad \int_0^{t_{\text{total}}} f_{\text{cont}}(t)\, dt < \gamma, \tag{14}$$

where γ is some tolerance for variation. This is minimization problem is subject to a total variation constraint, which has been subject to considerable study, especially within the context of medical imaging [10].

This optimization leads to a natural discretization. We rewrite:

$$V(t) \longrightarrow V^t \tag{15}$$

$$\frac{dV}{dt} = c \longrightarrow V^{t+1} - V^t = c \tag{16}$$

$$f_{\text{cont}}(t) = \int_\Omega |T(x,y,t) - T_{\text{f}}| \; d\omega \longrightarrow f_{\text{disc}}(t) = \sum_{x,y} |T(x,y,t) - T_{\text{f}}|\,, \tag{17}$$

which translate to the problem

$$\arg\min_c \sum_{t=0}^{t_{\text{total}}} V^{t_{\text{total}}} \quad \text{such that} \quad \sum_{t=0}^{t_{\text{total}}} f_{\text{disc}}(t) < \gamma. \tag{18}$$

The minimization problem posed here captures the major features of the bathtub optimizer problem. In our problem, the bather need not frequently calibrate the settings of the bathtub; rather, the bathtub "policy" reduces to an initial choice of c. Moreover, the underlying objective is not to get an even temperature distribution (as the bather may simply leave the faucet on arbitrarily long to achieve this), but to conserve as much water as possible. The temperature distribution problem, then, must be seen within the framework of water conservation first and not vice versa. On the other hand, the best volume minimization policy is $c = 0$, so the bounded temperature total variation constraint incorporates the desired $c > 0$ aspects of the problem. Finally, from both a numerical perspective and a feasibility perspective, demanding complete temperature uniformity, $\gamma = 0$, is impossible. Instead, γ represents the degree of tolerance to which the bather can expect a range of temperatures in the bathtub.

3. Empirical results

Our work is highly preliminary and requires more study in order to better calibrate our models and properly run experiments. However, we simulated a number of variously parametrized situations and can report on the model as a proof of concept.

Figure 1: The heat diffusion process in the case of a stationary fluid and constant faucet tap. The mesh dimensions are 50×50, $\alpha = 10^{-3}$, $T_{\text{tub}} = 10$, and $T_{\text{faucet}} = 30$.

For example, the above figure shows a heat-diffusion process on a stationary fluid. The white ellipsoid in the left side of the image represents temperature emanating from the faucet source. Since the faucet water temperature is greater than the rest of the bathtub water, we observe temperature diffusion across the bathtub over time.

The same configuration yields a decreasing total variation of temperature as a function of time, which corroborates with the intuition that heat diffusing from a source increases the uniformity of the bathtub heat.

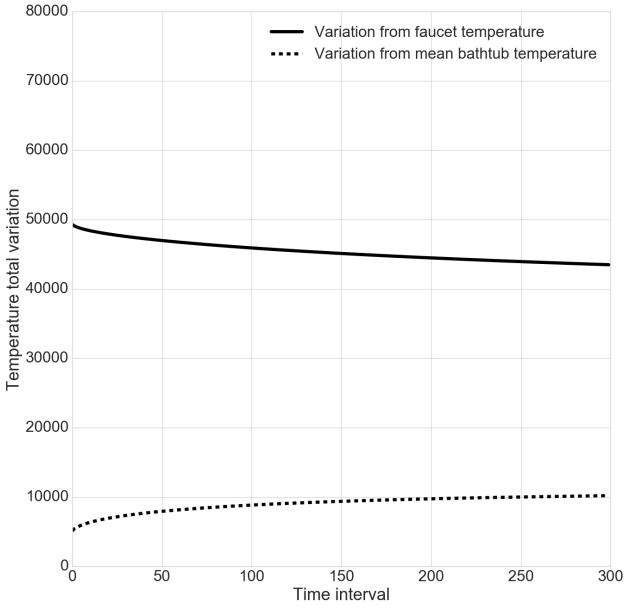

Figure 2: Temperature total variation over time in the case of a stationary fluid, with the same parameters as in Figure 1. The monotonicity of the TV function is in line with basic intution.

We can also examine the case in which the faucet water is turned on only for the initial instant. Our proposed optimization model omits this possibility since it requires a fixed water flux from the faucet. However, when we formulated the model we relied on the intuitive justification that the overall temperature would diverge from the faucet temperature. We simulate the heat diffusion in a stationary fluid for which the "faucet" turns off immediately after the outset of the simulation.

Figure 3: The heat diffusion process in the case of a stationary fluid and temporary faucet tap. The mesh dimensions are 50×50, $\alpha = 10^{-3}$, $T_{\text{tub}} = 10$, and $T_{\text{faucet}} = 30$.

We see the overall temperature level decreases rapidly after the first time interval, but the uniformity increases. However, as we modeled total variation as deviation from the faucet temperature, we see that the total variation receives a higher penalty than before.

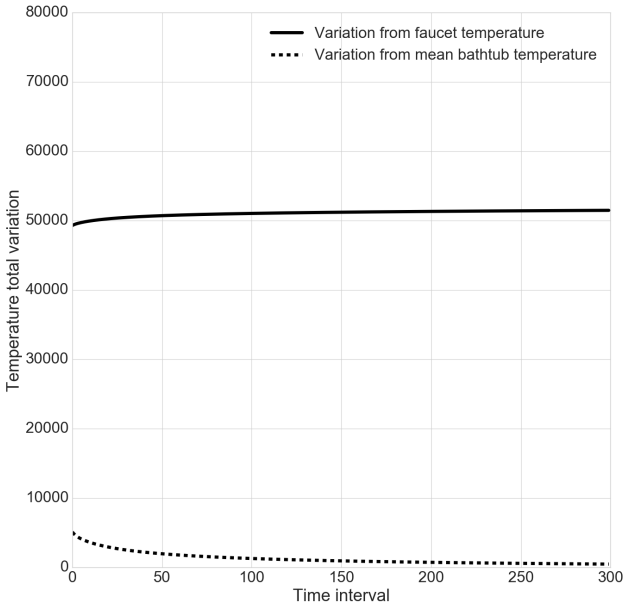

Figure 4: Temperature total variation over time in the case of a stationary fluid, with the same parameters as in Figure 3. The monotonicity of the TV function is in line with basic intution.

The fact that the total variation performs so poorly in this case has implications for the policy problem, which we will discuss in the next section.

Generalizing beyond stationary fluids reveals a number of critical issues of the numerical techniques employed in this study, but also provides useful information regarding the underlying problem. In stationary fluid, the Navier-Stokes and Poisson equations are not in play; however, by relaxing the stationarity constraint, we observe the effects fluid flow on the diffusivity of heat. We simulate the case described in Figure 1 but relax the stationarity constraint.

Figure 5: The heat diffusion process in the case of a moving fluid and permanent faucet tap. The mesh dimensions are 50×50, $\alpha = 10^{-3}$, $T_{\text{tub}} = 10$, and $T_{\text{faucet}} = 30$. The parameter controlling the fluid motion is set $b = 5$.

By comparing Figure 5 with Figure 1, we see that adding the convection process into the model actually improves the spread of the faucet temperature. Since more of the bathtub area is white in the images, we have more of the surface area heated by the temperature water. This phenomenon is confirmed by measuring the total variation of the bathtub water over time.

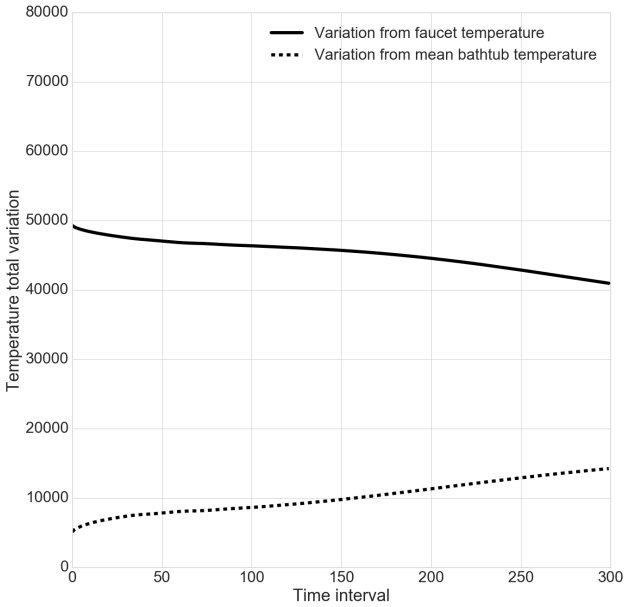

Figure 6: Temperature total variation (with respect to T_{faucet} and with respect to the mean bathtub temperature over time in the case of a nonstationary fluid, with the same parameters as in Figure 5. The TV functions are considerably less well behaved, but notably the TV with respect to T_{faucet} decreases to a lower level than the same TV in Figure 2.

There are three interesting phenomena present in this result. First, we see that the evolution of the total variation over time is less well-behaved than before. We also note that the total variation with respect to the mean bathtub temperature grows almost linearly with time and exhibits much less concavity than Figure 2. Finally, the total variation with respect to T_{faucet} reaches a lower threshold than the total variation in the diffusion case only in Figure 2.

The choice of $b = 5$ is essntially arbitrary; however the behavior of the fluid with respect to different choices is highly volatile. In fact, modest changes to the value for b have drastic implications for the numerical stability of the fluid flow, and consequently the temperature. We see this phenomenon in Figures 7 and 8.

Figure 7: The heat diffusion process in the case of a moving fluid and permanent faucet tap. The mesh dimensions are 50×50, $\alpha = 10^{-3}$, $T_{\text{tub}} = 10$, and $T_{\text{faucet}} = 30$. The parameter controlling the fluid motion is set $b = 8$. The numerical instability of the simulation causes the complete whitewashing by the final frame.

The evolution of frames in Figure 7 represents an explosion in the numerical values associated with the temperatures. The black-white ridge in the bottom right corner of the third frame exhibits the typical instability phenomenon we observed in the simulations. Emanating from near the faucet source, this phenomenon appears to push out towards the boundary

of the frame until the entire frame is whitewashed. We can also see this last-minute explosion by measuring the total variation.

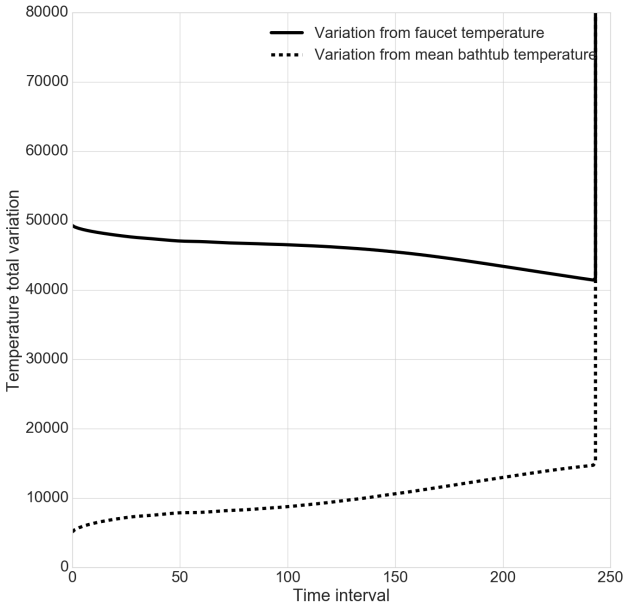

Figure 8: Temperature total variation (with respect to T_{faucet} and with respect to the mean bathtub temperature over time in the case of a nonstationary fluid, with the same parameters as in Figure 5. The TV functions are considerably less well behaved, but notably the TV with respect to T_{faucet} decreases to a lower level than the same TV in Figure 2.

The presence of a constant heat and flow source in the faucet might suggest that the numerical instability associated with the parametrization of b relates also to the source. We see that this is not the case. The numerical instability persists even when the faucet is turned off, as in Figure 3.

Figure 9: The heat diffusion process in the case of a moving fluid and temporary faucet tap. The mesh dimensions are 50×50, $\alpha = 10^{-3}$, $T_{\text{tub}} = 10$, and $T_{\text{faucet}} = 30$. The parameter controlling the fluid motion is set $b = 8$. The numerical instability of the simulation causes the complete whitewashing by the final frame.

Interestingly, the second frame seems to show numerical instability towards underflow, but by the third frame we observe near complete whitewashing of the same characterization as Figure 7. We also see the black-white ridge in the bottom right corner of the third frame, again in a similar fashion to Figure 7.

More surprisingly is the behavior of the temperature total variation, as we see below in Figure 10.

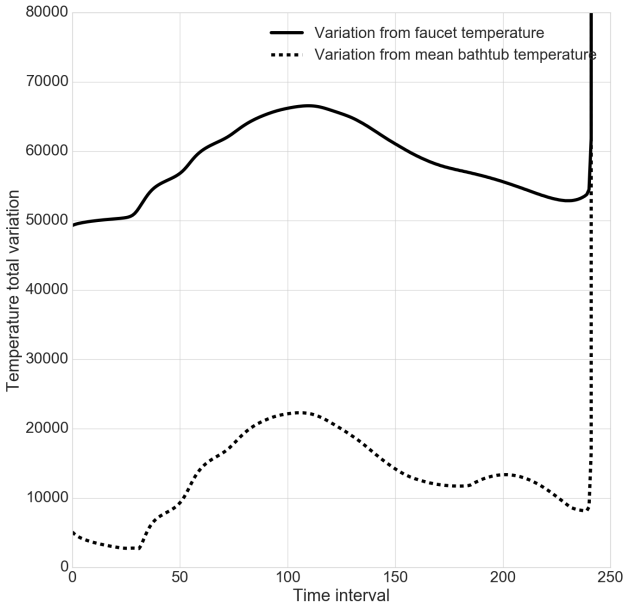

Figure 10: Temperature total variation (with respect to T_{faucet} and with respect to the mean bathtub temperature over time in the case of a nonstationary fluid, with the same parameters as in Figure 9. The TV functions are very poorly behaved and exhibit no similar characteristics to the previous configurations of the simulation.

We have no intuition or explanation for the behavior of these total variation functions. We suspect that this is almost entirely due to numerical artifacts in the simulation but cannot speak with any authority to why the hump shape appears in the plots. We do note, however, that the hump appears to correspond to the second frame of Figure 9, in which we observe a very dark region with low temperature.

4. Discussion

As we showed in the previous section, our current numerical implementation of the Navier-Stokes equations are highly sensitive to the initial conditions of the model. Though a careful calibration of the deep parameters (e.g. ρ, α, b, etc.) and mesh granularity might produce more stable results, we doubt that this would be sufficient. Fundamentally, forward Euler approximations of the solutions to differential equations encourage volatility by accumulating the relatively small errors from the individual step calculations into catastrophically unstable general results. To prevent this kind of instability requires a re-examination of the numerical approach to approximating these PDEs.

Perhaps somewhat surprising, then, is the fact that diffusion alone seems to abstain from these stability problems. Indeed, if numerical differentiation is the problem, then diffusion, which computes the Laplacian, should produce even greater error. However, due to the simplicity of the stability conditions for diffusion (for example, see Barba's discussion [5]), the checks on stability can be readily accounted for and poor configuration choices can simply be avoided. This was the approach of the study. From a cursory glance at the Navier-Stokes and Poisson equations we understand that the stability conditions are not necessarily so simple, but incorporating them should help improve the reliability of the model.

That maintaining an active source (in the case of the bathtub narrative, a running faucet) reduces the total variation of the temperature in the bathtub supports our formulation of the

optimization problem and also indicates suitable choices for γ. Since including nonstationarity reduces the total variation of the temperature the farthest, we can suggest to the avid bather that keeping the water moving in the bathtub likely keeps the bathtub temperature more evenly distributed than letting the water approach stationarity.

Further investigation should attempt to mitigate the detrimental effects of unchecked numerical instability. The mesh approach to the numerical approximation of PDE solutions can be optimized [2, 5] to minimize the accumulation of error. Solving our proposed optimization problem requires additional study, too. Ultimately, our avid bather needs a policy to maximize her utility, so specifying the ideal velocity c remains the future priority.

References

[1] William F. Ames. *Numerical Methods for Partial Differential Equations*. 11 Fifth Avenue, New York, New York 10003: Academic Press,Inc., 1977.

[2] David Betounes. *Partial Differential Equations for Computational Science*. Springer-Verlag New York, Inc, 1998.

[3] *Convection-diffusion equation*. URL: https://en.wikipedia.org/wiki/Convection-deffusion_equation.

[4] D.g.Stephenson. "A Procedure for Determining the Thermal Diffusivity of Materials." In: *Journal of Building Physics* (1987). URL: http://jen.sagepub.com/content/10/4/236.abstract.

[5] Lorena A. Barba group. *CFD Python: 12 steps to Navier-Stokes*. URL: http://lorenabarba.com/blog/cfd-python-12-steps-to-navier-stokes/.

[6] L. D. Landau and E. M. Lifshitz. *Fluid Mechanics*. 2nd edition. Maxwell House, Fairview Park, Elmsford, New York 10523, U.S.A: Pergamon Press, 1987.

[7] *Physical properties of sea water 2.7.9*. URL: http://www.kayelaby.npl.co.uk/general_physics/2_7/2_7_9.html.

[8] *Thermal diffusivity*. URL: https://en.wikipedia.org/wiki/Thermal_diffusivity.

[9] The Engineering Toolbox. *Dry Air Properties*. URL: http://www.engineeringtoolbox.com/dry-air-properties-d_973.html (visited on 01/30/2016).

[10] Xiao-Qun Zhang and Jacques Froment. "Energy Minimization Methods in Computer Vision and Pattern Recognition: 5th International Workshop, EMMCVPR 2005, St. Augustine, FL, USA, November 9-11, 2005. Proceedings." In: ed. by Anand Rangarajan, Baba Vemuri, and Alan L. Yuille. Berlin, Heidelberg: Springer Berlin Heidelberg, 2005. Chap. Constrained Total Variation Minimization and Application in Computerized Tomography, pp. 456–472. ISBN: 978-3-540-32098-2. DOI: 10.1007/11585978_30. URL: http://dx.doi.org/10.1007/11585978_30.